Full Paper

Propellants, Explosives, Pyrotechnics

DOI: 10.1002/prep.201800281

A Rapid and Sensitive Quantitative Analysis Method for TNT using Raman Spectroscopy

Feng Gao,[a] Wenfang Liu,*[a] Zihui Meng,*[a] Pengfei Su,[b] Zhixue Li,[c] and Minghui Wang[c]

Abstract: Raman spectroscopy as a rapid and sensitive qualitative detection method has been applied in many fields; however, it is rarely used for the quantitative purpose due to poor reproducibility of peak area. Here, 2,4,6-trinitrotoluene (TNT) and its two byproducts, 2,4-dinitrotoluence (DNT) and 2,6-DNT, were firstly qualitatively analyzed by Raman spectroscopy and the characteristic parameters were extracted. Then, in the range of 2%–9% and 10%–90%, the standard curves were established between the area ratio of the characteristic peaks and the content of 2,4-DNT or 2,6-DNT using silver nanoflowers as the enhancing substrate. The fitting correlation for TNT/2,4-DNT or TNT/2,6-DNT system is around 0.99. The peak area ratio of the components exhibits much better dada reproducibility than peak area, and the relative error does not exceed 9.3% for at least six groups of parallel experiments.

Keywords: Raman spectroscopy · Quantitative analysis · TNT · 2,4-DNT · 2,6-DNT

1 Introduction

Raman spectroscopy is a molecular spectroscopy technique that can obtain information about the structure and functional groups of materials. Since the Raman activity corresponds to the change in the polarizability rather than the dipole moment when the molecule vibrates, some information that cannot be detected by infrared spectroscopy can be well represented in the Raman spectrum [1]. Compared with conventional analytical methods, Raman spectroscopy has the advantages of non-destructive, rapid, no special requirements for sample preparation, and can be used for trace analysis [2, 3]. Therefore, it has important application prospects in the analysis of food [4] and medicine [5], detection of microbial metabolic processes [7], diagnosis of basic microorganisms and DNA bases [9], and biomedical research [6]. And it is very sensitive to the conformation of polymer chains and the interactions between chains, providing information on the physicochemical properties of polymer [10–12]. In addition, it has also been widely used in the analysis and detection of explosives [8, 13, 14], especially for the identification of trace amounts of residues [15, 16]. However, most studies focus on the qualitative detection of compounds, a quantitative analysis via Raman spectroscopy is rarely reported.

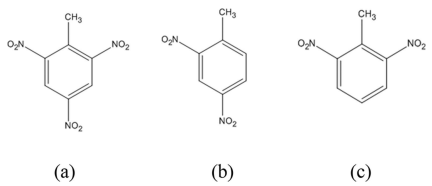

Figure 1. Structural formulas of TNT (a), 2,4-DNT (b), 2,6-DNT (c).

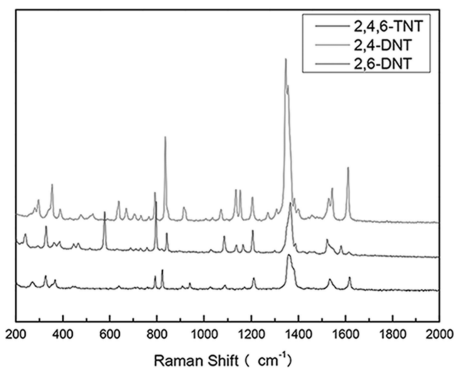

Figure 2. Raman spectra of TNT, 2,4-DNT and 2,6-DNT.

2,4,6-Trinitrotoluene (TNT) is a classic explosive that has been extensively used [17–19]. It is usually synthesized by the nitration of toluene, in which the byproducts such as

[a] *F. Gao, W. Liu, Z. Meng*
School of Chemistry and Chemical Engineering
Beijing Institute of Technology
Beijing 102488, China
**e-mail: liuwenfang@bit.edu.cn*
mengzh@bit.edu.cn
[b] *P. Su*
Xi'an Modern Chemistry Research Institute
Xi'an 710075, China
[c] *Z. Li, M. Wang*
Liaoning Qingyang Special Chemical Co., Ltd.
Wensheng District, Liaoyang 111002, China

Table 1. Comparison of the measured values of characteristic peaks of TNT, 2,4-DNT and 2,6-DNT with the literature.

Name	Measured value (cm^{-1})	Literature value (cm^{-1})
TNT	1621, 1537, 1362, 1215, 1088, 940, 823, 796, 366, 326	1616, 1533, 1357, 1209, 1086, 937, 821, 790, 636, 364, 324 [23]
2,4-DNT	1615, 1547, 1532, 1157, 838, 670, 389, 355	1605, 1550, 1510, 1152, 840 [24]
2,6-DNT	1582, 1526, 1370, 1209, 1140, 842, 799, 578, 387, 224	1582, 1533, 1375, 1204, 1138, 844, 796, 580, 391, 225 [25]

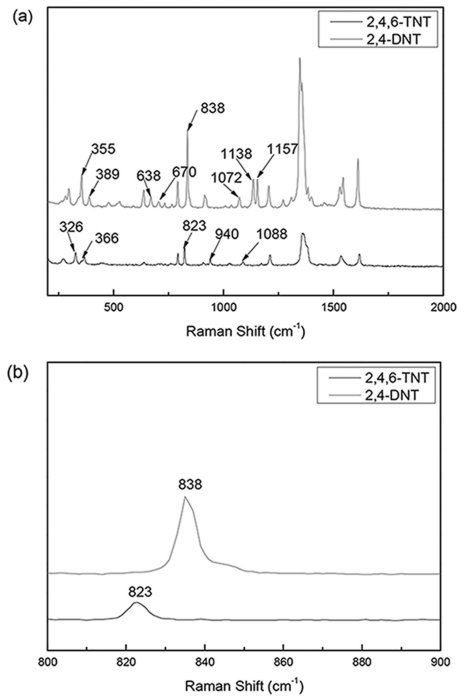

Figure 3. Full view (0–2000 cm^{-1}) (a) and partial enlargement (b) for Raman spectra of TNT and 2,4-DNT.

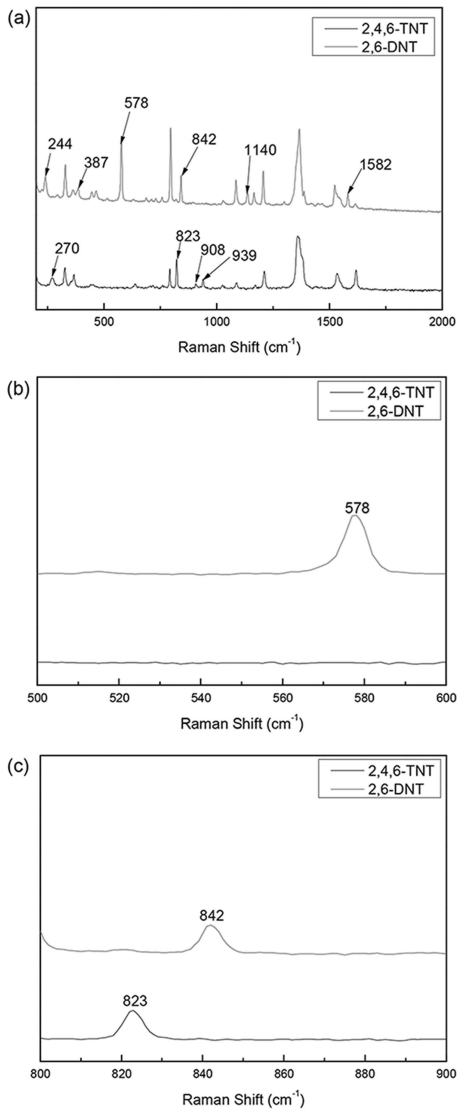

Figure 4. Full view (0–2000 cm^{-1}) (a) and partial enlargements (b–c) for Raman spectra of TNT and 2,6-DNT.

2,4-dinitrotoluence (DNT) and 2,6-DNT would be produced. In general, the purity of explosives has a great influence on their detonation and power [20, 2]. Liquid chromatography is a common approach for components analysis; nevertheless, it is very time-consuming and captious to separation conditions. In recent years, fluorescent sensor, ion mobility spectrometry and other technologies have been applied to qualitative and quantitative analysis of explosives. Although they have the advantages of high sensitivity and low detection limit, the preparation process is complicated [21, 22]. In this study, TNT, 2,4-DNT and 2,6-DNT were firstly evaluated qualitatively by Raman spectroscopy to find out their characteristic peaks. Then, the mixture of 2,4-DNT/TNT and 2,6-DNT/TNT with the different content of DNT were analyzed quantitatively with silver nanoflowers as the enhancing substrate. Taking the area ratio of the peaks of two components as the characteristic parameter, the corresponding standard curves were obtained in the range of 2%–9% and 10%–90%, and a quantitative analysis method for TNT was thereby established.

2 Experimental Section

2.1 Materials

Polyvinylpyrrolidone (PVP, 99%) was purchased from Beijing Bellingway Technology Co., Ltd. L-ascorbic acid (99%) was from Shanghai Dibo Biological Technology Co., Ltd. Silver nitrate (99.8%) was manufactured by Tianjin Fuchen Chemical

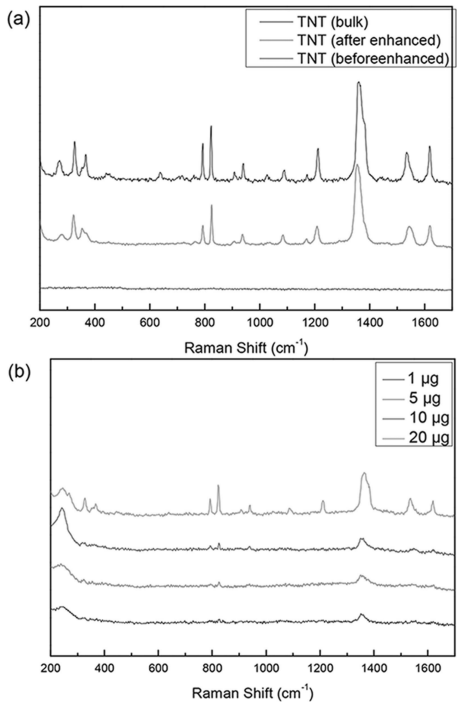

Figure 5. Raman spectra of TNT sample (45.6 μg) prepared from the solution before and after enhancement, and TNT bulk (a), and different amounts of TNT after enhancement (b).

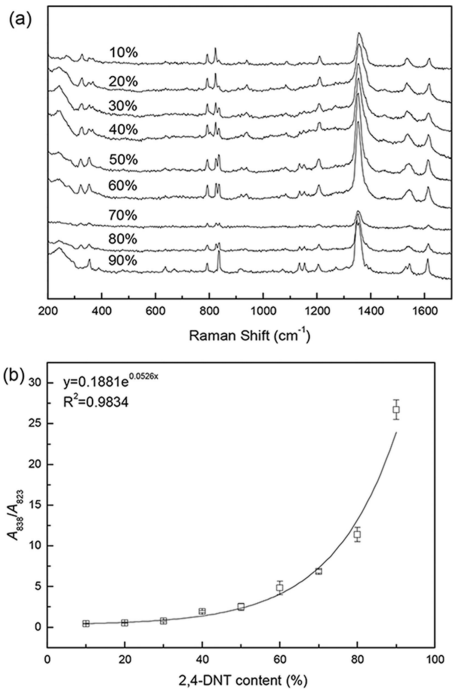

Figure 7. Raman spectra of 2,4-DNT/TNT system with 2,4-DNT content of 10 %–90 % (a), fitted curve of A_{838}/A_{823} with 2,4-DNT content (b).

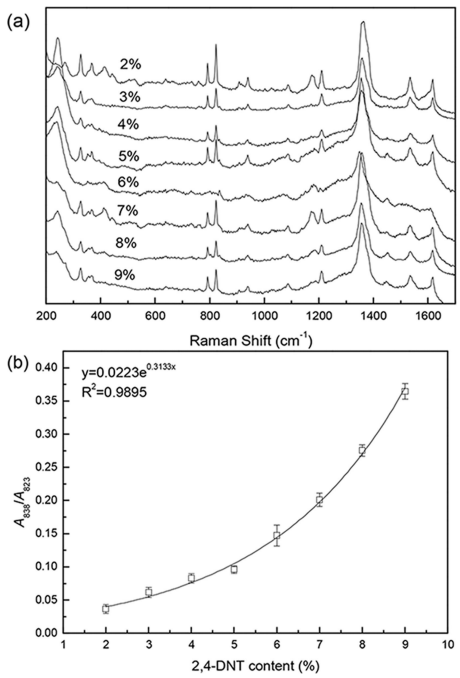

Figure 6. Raman spectra of 2,4-DNT/TNT system with 2,4-DNT content from 2 % to 9 % (a), fitted curve of A_{838}/A_{823} with 2,4-DNT content (b).

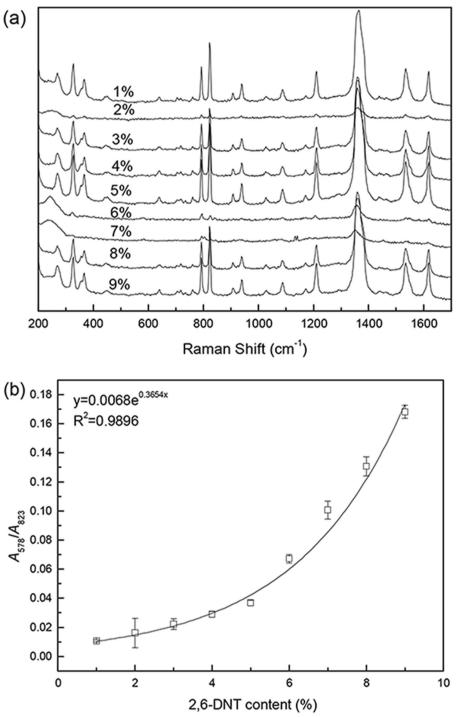

Figure 8. Raman spectra of 2,6-DNT/TNT system with 2,6-DNT content of 1 %–9 % (a), fitted curve of A_{578}/A_{823} with 2,6-DNT content (b).

Table 2. A_{838} and A_{838}/A_{823} values of 2,4-DNT/TNT system with 2,4-DNT content of 2%–9%.

Parallel experiment	2%		3%		4%		5%	
	A_{838}	A_{838}/A_{823}	A_{838}	A_{838}/A_{823}	A_{838}	A_{838}/A_{823}	A_{838}	A_{838}/A_{823}
1	264.7	0.0381	514.7	0.0643	313.7	0.0877	521.5	0.1050
2	162.3	0.0383	213.6	0.0650	331.6	0.0890	257.8	0.1020
3	195.6	0.0378	447.8	0.0648	425.7	0.0882	287.8	0.0998
4	98.21	0.0353	203.3	0.0611	155.3	0.0762	143.3	0.0892
5	201.2	0.0399	135.4	0.0704	99.82	0.0799	112.4	0.0902
6	199.3	0.0372	140.2	0.0636	233.4	0.0877	165.5	0.0987
7	99.82	0.0453	103.2	0.0552	88.40	0.0821	95.33	0.0922
8	30.49	0.0210	230.1	0.0450	235.6	0.0680	375.0	0.0890
9	99.87	0.0352	112.8	0.0627	102.8	0.0845	221.0	0.0968
$\bar{X}$	150.2	0.0374	233.4	0.0636	220.7	0.0844	242.2	0.0959
S	68.70	0.0062	139.9	0.0069	112.4	0.0066	130.3	0.0056
Z (%)	8.1–79.7	3.3–9.3	1.5–121	0.3–6.0	5.8–92.9	0.6–7.7	6.4–115	0.9–7.7
Parallel experiment	6%		7%		8%		9%	
	A_{838}	A_{838}/A_{823}	A_{838}	A_{838}/A_{823}	A_{838}	A_{838}/A_{823}	A_{838}	A_{823}/A_{823}
1	660.7	0.1510	101.7	0.1920	180.8	0.2780	155.5	0.3630
2	459.9	0.1630	203.1	0.2100	192.4	0.2850	188.9	0.3620
3	456.0	0.1580	198.8	0.2030	233.4	0.2710	331.5	0.3610
4	334.5	0.1430	203.4	0.1870	184.5	0.2680	209.9	0.3490
5	233.1	0.1550	179.9	0.2210	222.4	0.2770	189.2	0.3520
6	143.3	0.1520	358.4	0.1990	184.3	0.2640	305.6	0.3710
7	49.45	0.1390	83.90	0.2210	115.3	0.2890	154.2	0.3820
8	83.89	0.1100	95.33	0.1940	180.9	0.1990	256.3	0.3580
9	158.9	0.1550	146.8	0.2010	133.2	0.2720	165.6	0.3820
$\bar{X}$	286.6	0.1523	174.6	0.2000	180.8	0.2755	217.4	0.3640
S	193.8	0.0016	79.30	0.0095	35.30	0.0252	61.90	0.0111
Z (%)	22.9–131	2.9–6.1	2.9–105	0.05–4	0.02–56.8	1.1–8.2	3.4–52.5	0.38–4.8

Reagent Factory. TNT was provided by Liaoning Qingyang Special Chemical Co., Ltd. 2,4-DNT and 2,6-DNT with a purity of 99% were produced by Xi'an Modern Chemistry Research Institute. Methanol and ethanol in analytical grade were purchased from Beijing Chemical Factory.

2.2 Preparation of Silver Nanoflowers

Silver nanoflowers were prepared referring to the reported method [3]. Firstly, 10 mL ultrapure water, 2 mL aqueous solution of PVP (1%) and 0.2 mL aqueous solution of silver nitrate (1 mol L^{-1}) were added into a clean beaker with magnetic stirring. Then, 1 mL aqueous solution of ascorbic acid (0.1 mol L^{-1}) was added dropwise to the above mixture. After stirring for 15 min, the resultant suspension was centrifuged at 5000 rpm for 10 min. The sediments were successively washed with ultrapure water and ethanol, and then stored in 20 mL ethanol for use.

2.3 Raman Spectroscopy Measurement

2.3.1 Qualitative Analysis

For a qualitative analysis of TNT, 2,4-DNT and 2,6-DNT, the sample powder was spread over a glass slide wrapped by the foil, then scanned with a portable Shimadzu Raman spectrometer Model OPAL 3000 in a spectrum range of 0–3250 cm^{-1}, with the exposure time of 1 s and scanning power of 100 mW.

To determine the detection limit for TNT with silver nanoflowers as the substrate, firstly, 20 μL suspension of silver nanoflowers in ethanol was added into an aluminum sample cell, after the solvent was volatilized, 20 μL methanol solution of TNT with different concentration was added, which was then left in a fume hood until dried. The blank experiment was also conducted under the same conditions except for no silver substrate.

2.3.2 Quantitative Analysis

In order to evaluate the purity of TNT using Raman spectroscopy, a series of solid mixture of TNT and 2,4-DNT (or 2,6-DNT) were prepared. The total mass of the mixture was

Table 4. A_{578}/A_{823} values of 2,6-DNT/TNT system with 2,6-DNT content of 1%–9%.

Parallel experiment	1%	2%	3%	4%	5%
1	0.0109	0.0125	0.0185	0.0270	0.0358
2	0.0124	0.0121	0.0192	0.0269	0.0347
3	0.0099	0.0410	0.0182	0.0274	0.0360
4	0.0105	0.0119	0.0213	0.0296	0.0355
5	0.0114	0.0133	0.0232	0.0331	0.0372
6	0.0105	0.0127	0.0232	0.0298	0.0363
7	0.0099	0.0115	0.0263	0.0287	0.0387
8	0.0107	0.0122	0.0278	0.0295	0.0401
$\bar{X}$	0.0108	0.0126	0.0214	0.0284	0.0363
S	0.0008	0.0095	0.0033	0.0019	0.0017
Z (%)	0.74–5.8	2.5–5.4	2.5–4.1	1.7–7.2	2.1–8.3
Parallel experiment	6%	7%	8%	9%	
1	0.0646	0.0908	0.1234	0.1690	
2	0.0652	0.0967	0.1255	0.1702	
3	0.0660	0.1030	0.1321	0.1660	
4	0.0643	0.0982	0.1247	0.1690	
5	0.0675	0.0996	0.1302	0.1590	
6	0.0673	0.1040	0.1312	0.1720	
7	0.0702	0.1010	0.1430	0.1660	
8	0.0725	0.1120	0.1360	0.1720	
$\bar{X}$	0.0672	0.1007	0.1290	0.1681	
S	0.0027	0.0058	0.0061	0.0042	
Z (%)	0.15–7.9	0.34–3.3	0.43–8.5	0.52–2.3	

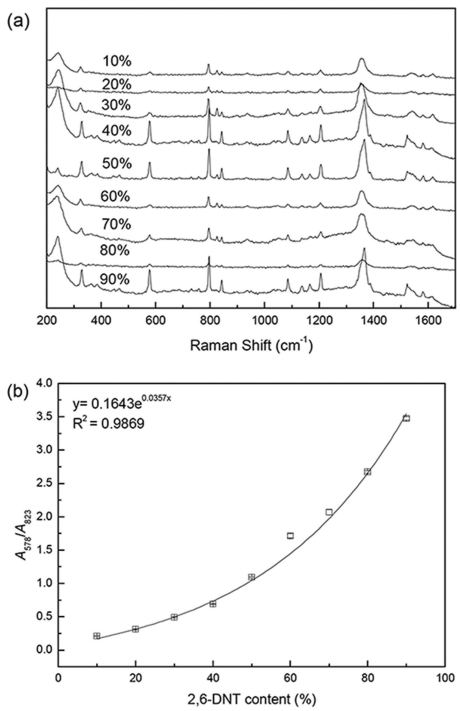

Figure 9. Raman spectra of 2,6-DNT/TNT system with 2,6-DNT content of 10%–90% (a), fitted curve of A_{578}/A_{823} with 2,6-DNT content (b).

Table 5. A_{578}/A_{823} values of 2,6-DNT/TNT system with 2,6-DNT content of 10%–90%.

Parallel experiment	10%	20%	30%	40%	50%
1	0.221	0.312	0.498	0.691	1.098
2	0.198	0.305	0.503	0.683	1.069
3	0.203	0.324	0.489	0.688	1.093
4	0.198	0.317	0.502	0.685	1.097
5	0.220	0.312	0.491	0.683	1.096
6	0.212	0.307	0.496	0.693	1.112
7	0.224	0.295	0.514	0.688	1.099
8	0.209	0.304	0.489	0.686	1.096
9	0.227	0.319	0.478	0.702	1.103
10	0.213	0.317	0.487	0.699	1.087
$\bar{X}$	0.213	0.311	0.495	0.690	1.095
S	0.010	0.008	0.001	0.006	0.011
Z (%)	0.24–6.8	0.26–4.1	0.26–3.9	0.26–1.77	0.09–1.55
Parallel experiment	60%	70%	80%	90%	
1	1.703	2.066	2.677	3.423	
2	1.712	2.102	2.645	3.507	
3	1.707	2.072	2.663	3.452	
4	1.713	2.079	2.659	3.458	
5	1.698	2.081	2.665	3.465	
6	1.707	2.091	2.650	3.472	
7	1.806	2.125	2.700	3.510	
8	1.698	1.999	2.675	3.487	
9	1.692	2.013	2.705	3.484	
10	1.696	2.043	2.695	3.492	
$\bar{X}$	1.713	2.067	2.673	3.475	
S	0.032	0.037	0.020	0.025	
Z (%)	0.07–5.4	0.11–3.3	0.06–1.2	0.09–1	

100 mg, and the content of 2,4-DNT or 2,6-DNT was respectively 1%–9% and 10%–90%. The resultant mixture was dissolved in 10 mL methanol, and then 20 μL of the above solution was transferred into a sample cell coated by silver substrate. After dried, the sample was analyzed using Raman spectrometer.

The peak area was integrated using the Origin software. The standard deviation (S) was calculated based on the results of the parallel experiments according to Eq. (1), and the relative error (Z) was calculated according to Eq. (2). Where, X_i represents the measured value, $\bar{X}$ is the average value of all data in the parallel experiment except for the abnormal those (shaded), and N is the group number of the parallel experiments.

$$S = \sqrt{\frac{\sum_1^N (X_i - \bar{X})}{N-1}} \tag{1}$$

$$Z = \frac{X_i - \bar{X}}{\bar{X}} \times 100\,\% \tag{2}$$

3 Results and Discussion

3.1 Qualitative Analysis of TNT and DNT

The structural formulas of TNT, 2,4-DNT and 2,6-DNT are given in Figure 1. All of three contain Ar–NO_2, Ar–CH_3, and C–H, and their corresponding positions in the Raman spectrum are 1630–1500, 1360–1330 and 880–845 cm^{-1} for Ar–NO_2, 770–730 cm^{-1} for Ar–CH_3, and 1500–1300 cm^{-1} for C–H.

As shown in Figure 2, the characteristic peaks of TNT appear at 1621, 1362, 1537, 1215, 1088, 940, 823, 796, 366, 326 cm^{-1}, in which 1621, 1537 and 823 cm^{-1} can be assigned as the stretching vibration of Ar–NO_2, the peaks at 1362 and 1215 cm^{-1} are from C–H, the peak at 796 cm^{-1} is due to the stretching vibration of Ar–CH_3, the peaks at 366 and 326 cm^{-1} may be caused by the vibration of the C–C skeleton.

For 2,4-DNT, there are characteristic peaks at 1615, 1547, 1532, 1157, 838, 670, 389, 355 cm^{-1}. The peaks at 1615, 1547, 1532 and 838 cm^{-1} are presumed to be resulted from the presence of Ar–NO_2. The peak at 670 cm^{-1} is due to the stretching vibration of Ar–CH_3. The peaks at 389 and 355 cm^{-1} may be ascribed to the skeleton.

For 2,6-DNT, the characteristic peaks exist at 1582, 1526, 1370, 1209, 1140, 842, 799, 578, 387 and 224 cm^{-1}. The peaks at 1582, 1526 and 842 cm^{-1} are from Ar–NO_2, the peaks at 1370, 1209 and 1140 cm^{-1} are from C–H, and Raman peak of Ar–CH_3 appears at 799 cm^{-1}. The peak at 578 cm^{-1} may be caused by the stretching vibration of the benzene ring. Similarly, the peaks at 387 and 224 cm^{-1} are probably originated from the skeleton.

Table 1 lists the characteristic peaks of TNT, 2,4-DNT and 2,6-DNT. It can be seen that the measured values are very close to the reported those for all of them.

3.2 Extraction of Characteristic Parameters

In order to achieve quantitative analysis of TNT purity, the Raman spectra of TNT and 2,4-DNT (or 2,6-DNT) were compared to find out their respective characteristic peaks those did not overlap. Figure 3 gives full spectra (0–2000 cm^{-1}) of TNT and 2,4-DNT and a partial enlarged view. Compared with TNT, there are eight characteristic peaks in the Raman spectrum of 2,4-DNT, which are 1157, 1138, 1072, 838, 670, 638, 389 and 355 cm^{-1}. Among them, the peak at 838 cm^{-1} is the strongest. Compared with 2,4-DNT, TNT has characteristic peaks at 1088, 940, 823, 366, 326 cm^{-1}, in which the peak at 823 cm^{-1} is the strongest. Therefore, the Raman peaks at 838 cm^{-1} and 823 cm^{-1} were chosen for the quantitative analysis of the mixture of TNT and 2,4-DNT.

Figure 4 gives full spectra (0–2000 cm^{-1}) of TNT and 2,6-DNT and their partial enlarged views. Compared with TNT, there are six particular peaks for 2,6-DNT, which are 1582, 1140, 842, 578, 387 and 224 cm^{-1}. Compared with 2,6-DNT, TNT has four specific peaks at 939, 908, 823, and 270 cm^{-1}. Considering the intensity and shape of peak, the peak at 578 cm^{-1} for 2,6-DNT (Figure 4b) and 823 cm^{-1} for TNT (Figure 4c) was selected for the quantitative analysis of the mixture of TNT and 2,6-DNT.

3.3 Characterization of Silver Nanoflowers

In order to reduce the required sample amount in the quantitative analysis, the detect limit of Raman spectroscopy need be decreased. Therefore, low-cost silver nanoflowers with simple preparation process were used as the enhancing substrate in the following work. The Raman spectra of TNT sample prepared from the solution (see 2.3.1) before and after enhancement are compared in Figure 5a. It can be seen that with the same sample amount (45.6 μg), no signals were observed when no silver substrate, while the peaks were sharp and strong after enhancement. Although it was reported that silver substrate might change the peak position of the sample in some cases [18, 26], the positions of the peaks of TNT with silver enhancement were fundamentally the same as those of bulk sample (powder) in current study.

Further, the detect limit of Raman spectroscopy with silver nanoflowers as the enhancing substrate was measured in a range of 1–20 μg of TNT. It can be seen from Figure 5b, the detection limit was 5 μg. This work lays a vital basis for the following quantitative detection, in which the sample amount of 2,4-DNT or 2,6-DNT was 2–18 μg corresponding to a mass content of 1%–9%, and the lowest amount of TNT was 20 μg corresponding to 90% of DNT.

3.4 Quantitative Analysis of 2,4-DNT/TNT System

In a range of 1%–9% of 2,4-DNT, a mixed system of TNT and 2,4-DNT was analyzed via Raman spectroscopy. Figure 6a illustrates their spectra except for 1% of 2,4-DNT, for which the peak at 838 cm^{-1} is too weak to be integrated. As can be seen from the figure, the peak at 838 cm^{-1} arose with the increased content of 2,4-DNT, however, the peak intensity was not always related to the content level.

In order to examine the reproducibility of the peak area, A_{838}, and the area ratio of the peaks of 2,4-DNT and TNT, A_{838}/A_{823}, the dada of 9 groups of parallel experiments for different contents of 2,4-DNT are listed in Table 2. It can be seen that the standard deviation (S) and relative error (Z) of A_{838} were much higher than those of A_{838}/A_{823}. The value of A_{838} in the parallel experiment had poor repeatability and the Z value was in the range of 2%–130%. For A_{838}/A_{823}, the results of most parallel tests were relatively close except for the individual data (shaded), and the Z value did not exceed 9.3%.

These data were plotted against 2,4-DNT content. As shown in Figure 6b, an exponentially related curve was ob-

tained, and the expression was $y = 0.0223e^{0.3133x}$, and the fitting correlation was 0.9895.

In further, the 2,4-DNT/TNT system with a high 2,4-DNT content from 10% to 90% was also evaluated. Raman spectra are demonstrated in Figure 7a. Compared to Figure 6a, the peak of 2,4-DNT at 838 cm^{-1} was significantly enhanced. The A_{838}/A_{823} values of 9 groups of parallel experiments for different contents of 2,4-DNT are displayed in Table 3. It can be seen that except for the individual data (shaded), the results of most parallel tests were roughly the same, and the Z value was lower than 9%. Figure 7b gives the relation between of A_{838}/A_{823} and 2,4-DNT content, the regression equation was $y = 0.1881e^{0.0526x}$ with a fitting correlation of 0.9834.

Table 3. A_{838}/A_{823} values of 2,4-DNT/TNT system with 2,4-DNT content of 10%–90%.

Parallel experiment	10%	20%	30%	40%	50%
1	0.430	0.465	0.653	1.844	2.166
2	0.398	0.468	0.649	1.795	2.320
3	0.422	0.456	0.667	1.800	2.098
4	0.403	0.489	0.724	1.699	2.356
5	0.432	0.488	0.695	1.912	2.330
6	0.465	0.637	0.833	2.032	2.566
7	0.396	0.528	0.722	1.896	2.223
8	0.401	0.632	0.803	1.990	2.540
9	0.522	0.597	0.896	2.030	2.980
$\bar{X}$	0.419	0.486	0.685	1.853	2.357
S	0.039	0.070	0.082	0.106	0.252
Z (%)	0–2.9	1.7–8.6	4.2–5.7	0.31–8.3	1.1–8.9
Parallel experiment	60%	70%	80%	90%	
1	4.070	6.440	10.62	26.81	
2	3.990	6.580	11.02	28.07	
3	4.330	6.720	11.31	26.47	
4	4.523	6.823	11.21	26.58	
5	4.560	6.970	12.22	28.02	
6	4.783	7.040	11.98	27.76	
7	4.322	6.737	11.01	25.98	
8	5.120	7.080	13.22	26.73	
9	6.130	7.220	10.12	23.97	
$\bar{X}$	4.431	6.850	11.339	26.721	
S	0.618	0.238	1.133	1.191	
Z (%)	0.89–7.9	0.66–3.9	6.6–7.8	0.01–2.7	

3.5 Quantitative Analysis of 2,6-DNT/TNT System

The quantitative method using the area ratio of the characteristic peaks of two components was also examined in the 2,6-DNT/TNT system. Figure 8a shows Raman spectra of 2,6-DNT/TNT system with 2,6-DNT content varied from 1% to 10%. Although it is not easy to identify the peak of 2,6-DNT at 578 cm^{-1} and that of TNT at 838 cm^{-1} from full spectra, the integration results of peak area from the partial enlargement views of Raman spectra display that the area ratio of the peaks of 2,6-DNT and TNT, A_{578}/A_{823}, had good dada reproducibility for at least 7 groups of parallel experiments for different contents of 2,6-DNT, as listed in Table 4. The Z value was not above 8.5%. The standard curve is shown in Figure 8b, and A_{578}/A_{823} was exponentially correlated with 2,6-DNT content with an expression of $y = 0.0068e^{0.3654x}$ and a fitting correlation of 0.9896.

Figure 9a presents Raman spectra of 2,6-DNT/TNT system with a content of 2,6-DNT ranging from 10% to 90%. The peak of 2,6-DNT at 578 cm^{-1} was more pronounced than it was in low content of 2,6-DNT (Figure 8a). The A_{578}/A_{823} values of 10 groups of parallel experiments for different contents of 2,6-DNT are included in Table 5. Without eliminating any data, the relative error did not exceed 6.8%. The data of A_{578}/A_{823} was plotted against 2,6-DNT content. As shown in Figure 9b, the regression equation was $y = 0.1643e^{0.0357x}$, and the fitting correlation was 0.9869.

4 Conclusion

TNT, 2,4-DNT and 2,6-DNT were qualitatively analysed via Raman spectroscopy and their characteristic peaks were determined. With silver nanoflowers as the enhancing substrate, the detect limit of Raman spectroscopy for TNT was decreased to 5 μg, which made the following quantitative assay feasible with a greatly reduced sample amount.

Using the peak area ratio of 2,4-DNT and TNT, A_{838}/A_{823}, as the characteristic parameter, a standard curve was established in a range of 2,4-DNT content of 2%–9% and 10%–90%, the expression was $y = 0.0223e^{0.3133x}$ and $y = 0.1881e^{0.0526x}$, respectively. Similarly, the value of A_{578}/A_{823} was used for the content analysis of 2,6-DNT in the mixture of TNT and 2,6-DNT. The regression equation was $y = 0.0068e^{0.3654x}$ and $y = 0.1643e^{0.0357x}$, separately for 1%–9% and 10%–90% of 2,6-DNT.

This method has much better data reproducibility than peak area, and the relative error of 6–10 groups of parallel experimental data is within 9.3%. At the same time, it also exhibits outstanding regularity with the varied purity of TNT, and the fitting correlation is near 0.99.

Acknowledgement

This work was financially supported by the National Natural Science Foundation of China (U1530141).

References

[1] R. C. Lord, Introduction to Infrared and Raman Spectroscopy, *Academic. Press.* **1964**, 155–1156.

[2] H. Brust, S. Willemse, T. Zeng, M. Koeberg, A. vanderHeijden, A. Bolck, P. Schoenmakers, Impurity Profiling of Trinitrotoluene

Using Vacuum-Outlet Gas Chromatography-Mass Spectrometry, *J. Chromatogr. A.* **2014**, *A(1374)*, 224–230.
[3] Y. J. Ai, P. Liang, Y. X. Wu, Q. M. Dong, J. B. Li„ Y. Bai, B. J. Xu, Z. Yu, D. Ni, Rapid Qualitative and Quantitative Determination of Food Colorants by Both Raman Spectra and Surface-Enhanced Raman Scattering (SERS), *Food. Chem.* **2018**, *241*, 427–433.
[4] H. Fischer, Raman-Microscopy in Food Analysis, *Appl. Spectrosc. Rew.* **2010**, *106*, 446–448.
[5] C. C. Huang, Applications of Raman Spectroscopy in Herbal Medicine, *Appl. Spectrosc. Rew.* **2016**, *51*, 1–11.
[6] C. Otto, C. J. D. Grauw, J. J. .Duindam, N. M. Sijtsema, J. Greve, Applications of Micro-Raman Imaging in Biomedical Research, *J. Raman Spectroscopy.* **2016**, *28*, 143–150.
[7] D. Gao, X. Huang, Y. Tao, A Critical Review of NanoSIMS in Analysis of Microbial Metabolic Activities at Single-Cell Level, *Crit. Rev. Biotechnol.* **2015**, *36*, 1–7.
[8] M. López-López, C. García-Ruiz, Infrared and Raman Spectroscopy Techniques Applied to Identification of Explosives, *Trend. Anal. Chem.* **2014**, *54*, 36–44.
[9] C. Otto, V. Dttjj, D. M. Ffm, J. Greve, Surface-Enhanced Raman Spectroscopy of DNA Bases, *J. Raman Spectroscopy.* **2017**, 17(3), 289–298.
[10] J. Song, G. Niu, X. Chen, Amphiphilic-Polymer-Guided Plasmonic Assemblies and Their Biomedical Applications, *Bioconjugate Chem.* **2017**, *28*, 105–114.
[11] D. Garcia, Confocal Raman Spectroscopy and Principal Component Analysis of Multi-Layer Polymer Films, *ACS National Meeting Book of Abstracts.* **2007**, 233.
[12] F. T. C. Moreira, M. G. F. Sales, Smart Naturally Plastic Antibody Based on Poly(α-cyclodextrin) Polymer for β-Amyloid-42 Soluble Oligomer Detection. *Sensor, Actuat. B-Chem.* **2017**, *240*, 229–238.
[13] K. L. Gares, K. T. Hufziger, S. V. Bykov, S. A. Asher, Review of Explosive Detection Methodologies and the Emergence of Standoff Deep UV Resonance Raman, *J. Raman Spectroscopy.* **2016**, *47*, 124–141.
[14] D. S. Moore, R. J. Scharff, Portable Raman Explosives Detection, *Anal. Bioanal. Chem.* **2009**, *393*, 1571–1578.
[15] F. Zapata, M. López-López, C. García-Ruiz, Detection and Identification of Explosives by Surface Enhanced Raman Scattering, *Appl. Spectrosc. Rew.* **2016**, *51*, 227–262.
[16] A. Hakonen, P. O. Andersson, S. M. Stenbæk, T. Rindzevicius, M. Käll, Explosive and Chemical Threat Detection by Surface-Enhanced Raman Scattering: A Review, *Anal. Chim. Acta.* **2015**, *893*, 1–13.
[17] A. K. M. Jamil, A. Sivanesan, E. L. Izake, G. A. Ayoko, P. M. Fredericks, Molecular Recognition of 2,4,6-Trinitrotoluene by 6-Aminohexanethiol and Surface-Enhanced Raman Scattering Sensor, *Sensor Actuat B-Chem.* **2015**, *221*, 273–280.
[18] C. Zhang, K. Wang, D. Han, Q. Pang, Surface Enhanced Raman Scattering (SERS) Spectra of Trinitrotoluene in Silver Colloids Prepared by Microwave Heating Method, *Spectrochim. Acta.* **2014**, *122*, 387–391.
[19] K. L. Gares, S. V. Bykov, B. Godugu, S. A. Asher, Solution and Solid Trinitrotoluene (TNT) Photochemistry: Persistence of TNT-Like Ultraviolet (UV) Resonance Raman Bands, *Appl. Spectrosc.* **2014**, *68*, 49–56.
[20] C. N. Sheaff, D. Eastwood, C. M. Wai, R. S. Addleman, Fluorescence Detection and Identification of Tagging Agents and Impurities Found in Explosives, *Appl. Spectrosc.* **2008**, *62*, 739–746.
[21] X. S. Wang, L. Li, D. Q. Yuan, Y. B. Huang, R. Cao, Fast, Highly Selective and Sensitive Anionic Metal-Organic Framework with Nitrogen-Rich Sites Fluorescent Chemosensor for Nitro Explosives Detection, *J. Hazard. Mater.* **2017**, *344*, 283–290.
[22] H. Shahraki, M. Tabrizchi, H. Farrokhpor, Detection of Explosives Using Negative Ion Mobility Spectrometry in Air Based on Dopant-Assisted Thermal Ionization, *J. Hazard. Mater.* **2018**, *357*, 1–9.
[23] T. Liyanage, A. Rael, S. Shaffer, S. Zaidi, J. V. Goodpaster, R. Sardar, Fabrication of a Self-Assembled and Flexible SERS Nanosensor for Explosive Detection at Parts-per-Quadrillion Levels from Fingerprints, *Analyst.* **2018**, *143*, 2012–2022.
[24] J. M. Sylvia, J. A. Janni, J. D. Klein, K. M. Spencer, Surface-Enhanced Raman Detection of 2,4-Dinitrotoluene Impurity Vapor as a Marker to Locate Landmines, *Anal. Chem.* **2000**, *72*, 5834–5840.
[25] E. D. Emmons, J. A. Guicheteau, A. W. Fountain, S. D. Christesen, Comparison of Visible and Near-Infrared Raman Cross-Sections of Explosives in Solution and in the Solid State, *Appl. Spectrosc.* **2012**, *66*, 636–643.
[26] K. Kneipp, Y. Wang, R. Dasari, Near-Infrared Surface-Enhanced Raman Scattering of Trinitrotoluene on Colloidal Gold and Silver, *Spectrochimica Acta.* **1995**, *A(51)*, 2171–2175.

Manuscript received: September 17, 2018
Revised manuscript received: September 17, 2018
Version of record online: January 11, 2019

